

Effects of hydrogen plasma treatment on structural and optical properties of Ga₂O₃ sputtered films

JINGWEI DU¹, LEI FENG¹, TIANTIAN LI¹, JUN ZHU^{1,*}, SIHUA HA², HAI ZHANG²

¹*School of Physical Science and Technology, Inner Mongolia University, Hohhot 010021, People's Republic of China*

²*College of Sciences, Inner Mongolia University of Technology, Hohhot 010051, People's Republic of China*

The effects of hydrogen plasma treatment on the structural and optical properties of Ga₂O₃ thin films made by magnetron sputtering have been investigated in this work. Amorphous Ga₂O₃ films, which were sputtered at room temperature, will turn into β-Ga₂O₃ polycrystalline ones after thermal annealing in vacuum and the film crystallinity can be further improved by hydrogen plasma treatment. Because of the etching effect, the films became rougher leading to a little decrease of transmittance especially in the UV waveband. More oxygen vacancies were generated by hydrogen plasma as the temperature increases during plasma treatment. This study provides a means to achieve high-quality β-Ga₂O₃ ultraviolet transparent conductive films for optoelectronic device applications.

(Received November 22, 2022; accepted April 10, 2024)

Keywords: Ga₂O₃, Hydrogen plasma, Annealing, Transmittance

1. Introduction

In recent years, β-Ga₂O₃ with an ultra-wide bandgap of about 4.9 eV has received much attention due to its remarkable material properties and promising device applications in electronics and optoelectronics [1]. Although there are many methods reported to be used for preparing β-Ga₂O₃ thin films, magnetron sputtering is one of the most popular ones because it has advantages of low cost and low temperature deposition, and it can produce films with large area and high uniformity [2]. However, a Ga₂O₃ sputtered film, especially grown at room temperature (RT), is amorphous and behaves as an insulator [3]. It needs some post treatment strategies like annealing to enhance the film properties for further device fabrication.

Post annealing is always employed to improve the crystallinity of Ga₂O₃ thin films prepared not only by magnetron sputtering [4-6] but also by other methods [7-9]. In the annealing process, the samples are exposed in atmosphere with neutral atoms or molecules. The structural, morphological, as well as optical properties will be altered by adjusting the annealing temperature, time and ambient. Cha et al. [4] reported that annealing in a hydrogen atmosphere results in a direct conversion of β-Ga₂O₃ thin films to β-Ga₂O₃ nanowires. Hydrogen has proved to be an important impurity in oxide semiconductors where it can give rise to n-type conductivity and can also compensate deep acceptors [10]. Qin et al. [11] revealed that a number of additional hydrogen-containing defects are produced in β-Ga₂O₃ wafers annealing in a H₂ ambient. Theoretical calculations suggest that hydrogen in β-Ga₂O₃ should be a shallow donor and that interstitial hydrogen can also easily

form complexes with Ga vacancy acceptors V_{Ga}³⁻ that are major native defects in β-Ga₂O₃ [11, 12].

Except for annealing in H₂ ambient, hydrogen plasma treatment, where the samples are directly exposed in hydrogen plasma composed of lots of neutral atoms, molecules, active radicals, energetic ions and electrons [13], is another approach to introduce hydrogen in β-Ga₂O₃ and thus modulate its electric and optical properties. Polyakov et al. [14, 15] demonstrated that hydrogen plasma produces surface damage in the near-surface region and compensates shallow donors when studying the effect of hydrogen plasma on β-Ga₂O₃ epitaxial layers grown by halide vapor phase epitaxy (HVPE). The hydrogen plasma treatment was performed at an elevated temperature in an inductively-coupled plasma (ICP) reactor, flowed by a rapid thermal annealing in N₂ for 5min at 450 °C. In a later work, these authors observed an anisotropic plasma effect on bulk β-Ga₂O₃ crystals grown by edge-defined film-fed growth after hydrogen plasma treatment with the same conditions [16]. For the (-201) sample, hydrogen plasma exposure increased the net surface concentration of shallow donors. However, hydrogen plasma exposure of the (010) sample led to a strong decrease in the net shallow donor density.

However, hydrogen plasma treatment on Ga₂O₃ with other polymorphs like α-Ga₂O₃, κ-Ga₂O₃ and γ-Ga₂O₃ largely increases its n-type conductivity [17, 18]. Huynh et al. [19] studied the effects of remote hydrogen plasma treatment on β-Ga₂O₃ thin films prepared by pulsed laser deposition (PLD). They revealed that abundant hydrogen-related donors were formed at the near-surface region, accompanied by an enhancement in the electrical conductivity of the film by an order of magnitude. But the sheet resistance at RT was still very high (4×10⁸ Ω/sq) after

the hydrogen incorporation. Venzie et al. [20] studied the properties of impurity-hydrogen complexes in Si-doped Ga_2O_3 epitaxial layers grown by molecular beam epitaxy (MBE) and subsequently treated in hydrogen plasma. The influences of hydrogen plasma exposure on the electric and optical properties were also studied on the $\beta\text{-Ga}_2\text{O}_3$ heteroepitaxial thin films grown by low-pressure chemical vapor deposition (LPCVD) [21, 22]. However, there still lacks information on hydrogen plasma effect on Ga_2O_3 sputtered films with amorphous or polycrystalline phase.

In this paper, we studied the effect of hydrogen plasma treatment on Ga_2O_3 sputtered films before and after thermal annealing. Different from ICP plasma, the hydrogen plasma of a relatively low ion density was excited by a capacitively-coupling plasma (CCP) apparatus equipped with a RF 13.56MHz power. There is no hydrogen-contamination in both sputtering and post annealing processes. This gives us convenience to discuss the change in structural and optical properties of Ga_2O_3 sputtered films due to hydrogen plasma treatment.

2. Experimental

Nominally undoped Ga_2O_3 thin films were deposited on double-sided polishing c-sapphire substrates by RF-magnetron sputtering at RT. Before being loaded into the sputtering chamber, the substrates were ultrasonically cleaned in an acetone bath to remove organic and metallic contaminants for 10 min, and ultrasonically cleaned successively in isopropyl alcohol for 10min, cleaned by deionized water and finally dried in a N_2 stream. A ceramic Ga_2O_3 target (99.99% purity) was used in a magnetron sputtering system which was equipped with a RF 13.56MHz power and can obtain a base vacuum of higher than 5×10^{-4} Pa. The target-to-substrate distance was set about 70 mm. Prior to deposition, the ceramic Ga_2O_3 target was pre-sputtered for 30 min to remove contaminants. The Ga_2O_3 thin films were then deposited with a RF power of 50 W at a working pressure of 0.2 Pa. The gas flow for Ar was in 30 sccm and for O_2 in 5 sccm. After sputtering, the samples were annealed at 700 °C in vacuum in a separate tubular furnace, in which the chamber pressure was controlled as 5×10^{-4} Pa, to avoid hydrogen-contamination and other impurity interruption. To investigate the influence from hydrogen plasma on Ga_2O_3 thin films with amorphous or polycrystalline phase, the hydrogen plasma treatment was performed before and after the annealing process. The H_2 flow was 50 sccm and working pressure was 173.3 Pa.

The surface morphology of Ga_2O_3 thin films was characterized by a field emission scanning electron microscope (SEM, SU8220, Hitachi). The crystal structure and phase of samples were characterized by an X-ray diffractometry (XRD) (Empyrean, Malvern Panalytical) with $\text{Cu-}\alpha$ ($\lambda = 0.154056$ nm) radiation. The element valence states were analyzed by an X-ray photoelectron spectrometer (XPS) (ESCALAB Xi+, Thermo Fisher). The

optical properties were studied by a UV-vis spectrophotometer (Lambda 750, PerkinElmer).

3. Results and discussion

In our experiment, Ga_2O_3 thin films were sputtered for 1 h and the film thickness was measured as approximately 120 nm by a step profiler (ET200A, Kosaka). Fig. 1 gives the SEM images of the as-sputtered Ga_2O_3 films after hydrogen plasma treatment using different RF power. It can be seen that the surface morphological change becomes more prominent as the power increases.

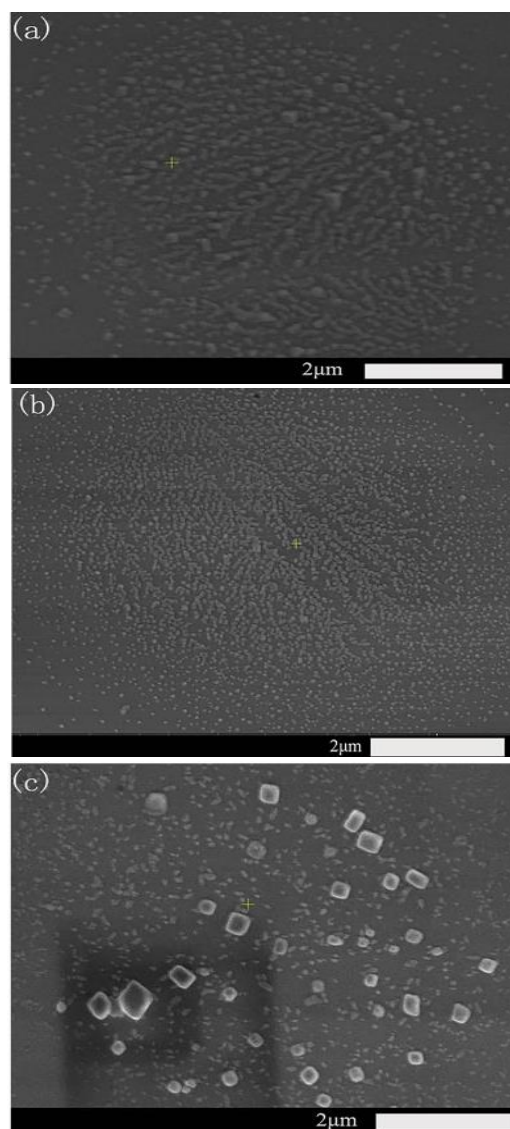


Fig. 1. SEM images of Ga_2O_3 films treated by hydrogen plasma at (a) 30 W, (b) 40W and (c) 50 W

When using 50 W, the calculated particle size ranges from 23.7 nm to 41.1 nm. Some bigger particles are observed possibly because of the stronger etching effect with increasing the power.

Fig. 2 gives XRD patterns of Ga₂O₃ sputtered films without and with vacuum annealing before treated by hydrogen plasma.

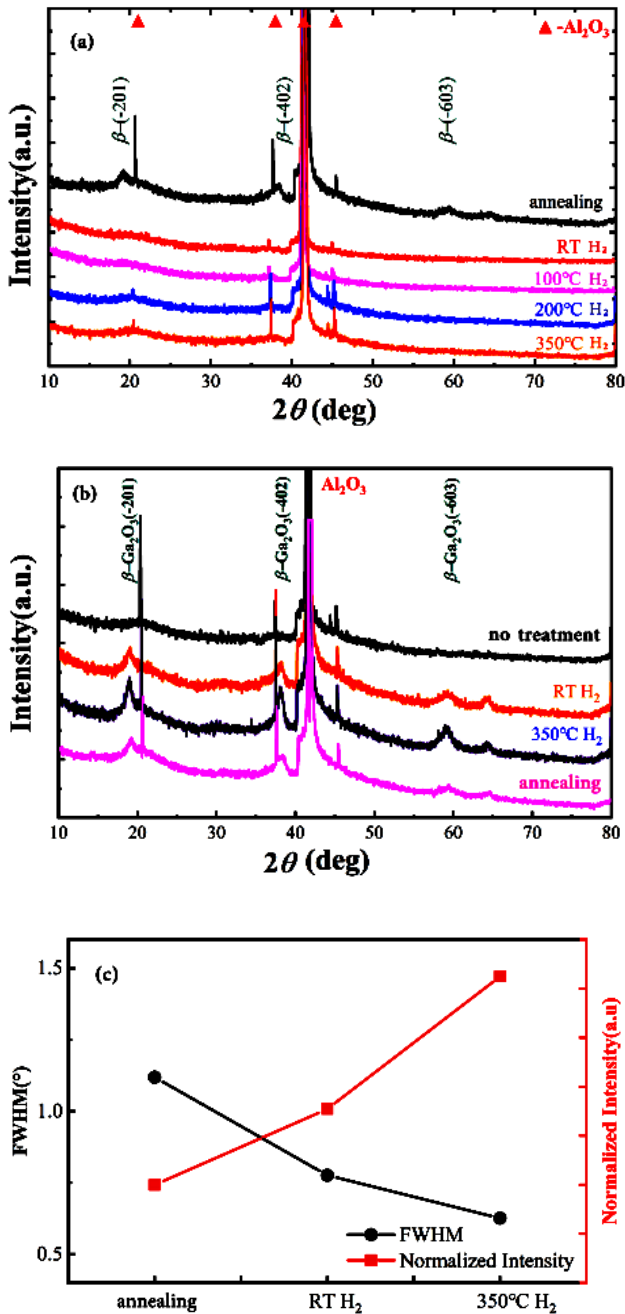


Fig. 2. XRD patterns of Ga₂O₃ films (a) without and (b) with annealing in vacuum before treated by hydrogen plasma at different temperature; (c) XRD FWHM and normalized intensity of Ga₂O₃ films (color online)

The hydrogen plasma treatment was performed with a power of 50 W for 10 min. It was observed from Fig. 2 (a) that there was no peak except for the substrate peaks with increasing the temperature of plasma treatment from RT to 350 °C. This indicates that without post annealing, the amorphous films could not turn into polycrystalline phase only by hydrogen plasma treatment. Post annealing process is more helpful in improving the film crystallinity. After vacuum annealing, Fig. 2 (b) shows three diffraction peaks nearly at $2\theta = 18.95^\circ$, 38.40° , and 59.19° , which are indexed as the (-201), (-402), and (-603) reflections of monoclinic β -Ga₂O₃ oriented along (-201) plane (JCPDS#43-1012). The calculated FWHM and integral intensity of (201) peak were given in Fig. 2 (c). It was shown that the peak became sharper and higher, indicating that the crystal quality and preferred orientation were further improved with increasing the temperature in hydrogen plasma treatment.

In order to study the changes in surface electronic states due to hydrogen plasma, the Ga₂O₃ annealed films after hydrogen plasma treatment were measured by XPS. The results for the Ga₂O₃ annealed film without plasma treatment were also depicted for comparison. Contaminants on the surfaces of the samples were cleaned by N₂ before measurement and the test results were calibrated by C 1s (284.8 eV). Fig. 3 (a) shows the XPS survey spectra of the Ga₂O₃ thin films. The characteristic peaks of Ga 3s, Ga 3p, Ga 3d and O 1s were clearly observed and there was no peak of other impurities, which indicates that only Ga and O exist in the films. After Gaussian fitting and peak decomposing, XPS spectra of O 1s core level with and without hydrogen plasma treatment are given in Fig. 3(b). Prior to hydrogen plasma treatment, no change was observed for O 1s peak resulting in nonstoichiometric Ga₂O₃ sputtered in O-rich atmosphere. There was only the characteristic peak of O-Ga bond at 531.5 eV (denoted as peak 1). It demonstrated that the lattice oxygen concentration did not change thus the crystal structure was not altered after thermal annealing in vacuum. Whereas, the peak 1 shows a redshift and the characteristic peak of O-H bond [20] at 532.5 eV (denotes as peak 2) appears after hydrogen plasma treatment, leading to more oxygen vacancies. This also suggests that plasma-induced hydrogen radicals are absorbed into β -Ga₂O₃ and form strong bonds with O atoms. The increased oxygen vacancies concentration will have an impact on the optical properties of Ga₂O₃ thin films.

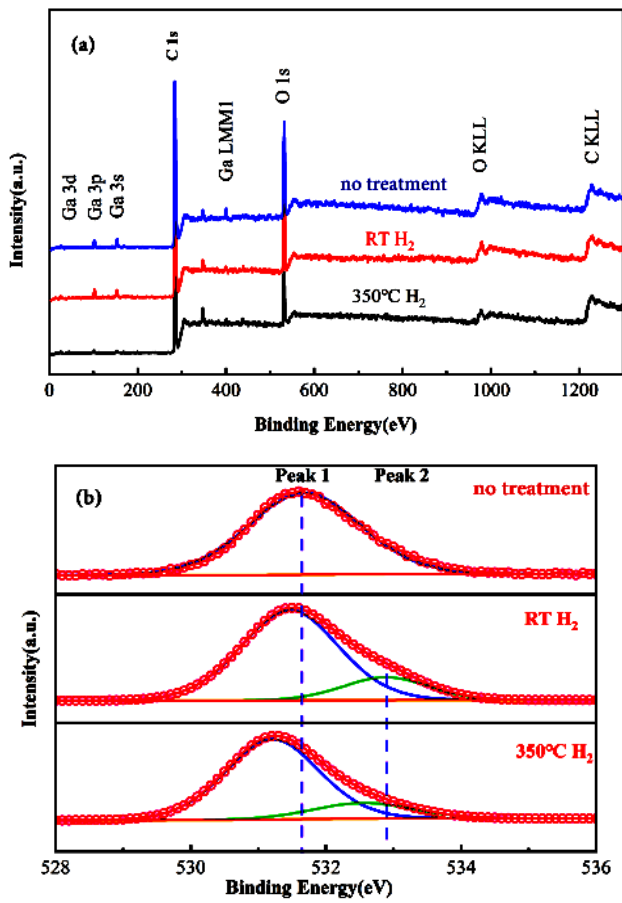


Fig. 3. (a) XPS survey spectra and (b) XPS spectra of O 1s core level of Ga_2O_3 film with annealing in vacuum before treated by hydrogen plasma (color online)

Fig. 4 (a) shows the transmittance spectra of Ga_2O_3 sputtered thin films with no post treatment, with only thermal annealing at 700 °C and with thermal annealing followed by hydrogen plasma treatment at RT and 350 °C. It was seen that the optical transmittance in UV waveband and visible region with wavelength ranging from 400 nm to about 520 nm decreases for the samples with post annealing and/or hydrogen plasma treatment. The optical transmittance at 500 nm and the average ultraviolet transmittance in the UV waveband from 200 nm to 400 nm of the film after annealing and plasma treatment at 350 °C was about 97.8% and 64.6% respectively. As plasma treated at elevated temperature, the transmittance drops more obvious at short waveband from 250 nm to 500 nm. These results were caused by the larger grain size after annealing and larger surface roughness made by hydrogen plasma.

Tauc curve of $(\alpha h\nu)^2$ versus incident photon energy ($h\nu$) was plotted in Fig. 4 (b).

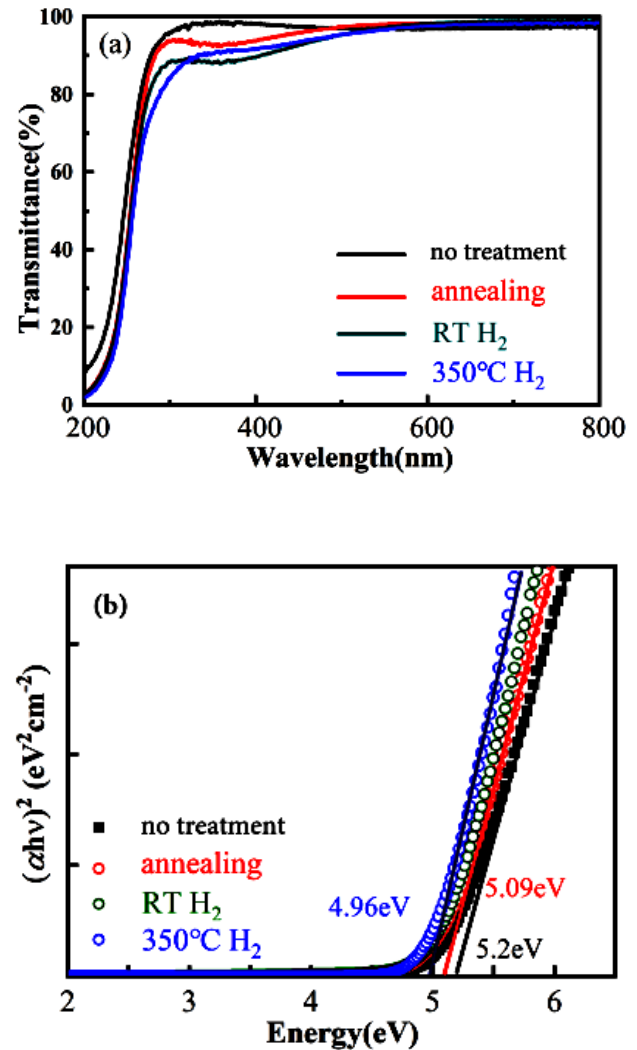


Fig. 4. (a) Transmittance spectra and (b) $(\alpha h\nu)^2$ versus photon energy $h\nu$ of Ga_2O_3 film with annealing in vacuum before treated by hydrogen plasma (color online)

The optical bandgap was calculated via Tauc formula [8] $(\alpha h\nu)^2 = \gamma(h\nu - E_g)$, in which ν is light frequency and γ is absorption edge width constant. α is wavelength dependent absorption coefficient which can be calculated by $\alpha = \frac{1}{t} \ln\left(\frac{1}{T}\right)$, where t is film thickness and T is optical transmittance. The optical bandgap of $\beta\text{-Ga}_2\text{O}_3$ annealed film was calculated as 5.09 eV. However, the optical bandgap was decreased about 1 eV by hydrogen plasma treatment. This observation is different from the result in [21]. On one hand, this was caused by light extinction since

the surface of Ga₂O₃ became rougher due to the physical bombardment of hydrogen plasma. On the other hand, according to the equation [23]

$$E_g(N) = \frac{3e^2}{16\pi\epsilon_s} \sqrt{\frac{Ne^2}{\epsilon_s kT}}$$

where N is the density of localized state, e is electronic charge, ϵ_s is the dielectric constant, k is Boltzmann's constant and T is the temperature, this decline may be caused by the increased density of localized state in conduction band due to more oxygen vacancies and hydrogen-related shallow donors. Unlike the conductive epitaxial films made by LPCVD [21, 22], our samples exhibit insulated regardless of annealing or/and plasma treatment when measured by a standard four-probe technique. It needs further doping other elements to substantially increase the electric conductivity of Ga₂O₃ sputtering films.

4. Conclusion

In conclusion, the Ga₂O₃ thin films were first deposited on c-sapphire substrates via RF-magnetron sputtering at RT and followed by vacuum annealing and hydrogen plasma treatment. The phase structure, elemental valence states and optical properties were analyzed by XRD, XPS and UV-vis spectra. Exposure in hydrogen plasma may cause three consequences: (1) surface damage caused by the physical bombardment from energetic particles; (2) surface local heating caused by the surface recombination of atomic hydrogen; (3) hydrogen-containing defects caused by hydrogen incorporation. The film crystallinity was improved by combination hydrogen plasma treatment with thermal annealing. Because of the etching effect, the films became rougher leading to a little decrease of transmittance especially in the UV waveband. However, the electric conductivity of Ga₂O₃ sputtered films was not improved prominently by H₂ plasma treatment. In order to get more evidences of hydrogen incorporation into Ga₂O₃ sputtered films and the hydrogen induced defect states by hydrogen plasma treatment, it is still necessary to utilize more measurements such as neutron reflectance spectra, deep level transient spectra and so on.

Acknowledgments

This work was supported by the National Natural Science Foundation of China (NNSFC) (Grant Nos. 62364014 and 12164031) and the Science Foundation of

Inner Mongolia Autonomous Region (Grant No. 2020MS06007).

References

- [1] C. Wang, J. Zhang, S. Xu, C. Zhang, Q. Feng, Y. Zhang, J. Ning, S. Zhao, H. Zhou, Y. Hao, J. Phys. D: Appl. Phys. **54**, 243001 (2021).
- [2] A. K. Saikumar, S. D. Nehate, K. B. Sundaram, ECS J. Solid State Sci. Technol. **8**, Q3064 (2019).
- [3] H. Liang, Z. Han, Z. Mei, Phys. Stat. Sol. A **218**, 2000339 (2021).
- [4] S. Y. Cha, B. -G. Ahn, H. C. Kang, S. Y. Lee, D. Y. Noh, Ceram. Int. **44**, 16470 (2018).
- [5] S. Jiao, H. Lu, X. Wang, Y. Nie, D. Wang, S. Gao, J. Wang, ECS J. Solid State Sci. Technol. **8**, Q3086 (2019).
- [6] Z. Chen, K. Ge, D. Meng, X. Chen, Mater. Lett. **320**, 132385 (2022).
- [7] F. Shi, J. Han, Y. Xing, J. Li, L. Zhang, T. He, T. Li, X. Deng, X. Zhang, B. Zhang, Mater. Lett. **237**, 105 (2019).
- [8] C. Wang, S. Li, Y. Zhang, W. Fan, H. Lin, D. Wu, S. Lien, W. Zhu, Vacuum **202**, 111176 (2022).
- [9] L. Gu, H. Ma, Y. Shen, J. Zhang, W. Chen, R. Yang, F. Wu, L. Yang, Y. Zeng, X. Wang, J. Zhu, Q. Zhang, J. Alloys Comp. **925**, 166727 (2022).
- [10] J. B. Varley, H. Peelaers, A. Janotti, J. Phys.: Condens. Matter **23**, 334212 (2011).
- [11] Y. Qin, M. Stavola, W. B. Fowler, P. Weiser, S. J. Pearton, ECS J. Solid State Sci. Technol. **8**, Q3103 (2019).
- [12] Y. Wei, X. Li, J. Yang, C. Liu, J. Zhao, Y. Liu, S. Dong, Sci. Rep. **8**, 10142 (2018).
- [13] I. Adamovich, S. Agarwal, E. Ahedo, L. L. Alves, S. Baalrud, N. Babaeva, A. Bogaerts, A. Bourdon, P. J. Bruggeman, C. Canal, E. H. Choi, S. Coulombe, Z. Donko, D. B. Graves, S. Hamaguchi, D. Hegemann, M. Hori, H. -H. Kim, G. M. W. Kroesen, M. J. Kushner, A. Laricchiuta, X. Li, T. E. Magin, S. M. Thagard, V. Miller, A. B. Murphy, G. S. Oehrlein, N. Puac, R. M. Sankaran, S. Samukawa, M. Shiratani, M. Simek, N. Tarasenko, K. Terashima, E. Thomas Jr, J. Trieschmann, S. Tsikata, M. M. Turner, I. J. van der Walt, M. C. M. van de Sanden, T. von Woedtke, J. Phys. D: Appl. Phys. **55**, 373001 (2022).
- [14] A. Y. Polyakov, I. Lee, N. B. Smirnov, E. B. Yakimov, I. V. Shchemerov, A. V. Chernykh, A. I. Kochkova, A. A. Vasilev, A. S. Shiko, Patrick H. Carey, F. Ren, S. J. Pearton, ECS J. Solid State Sci. Technol. **8**, P661 (2019).
- [15] A. Y. Polyakov, I. Lee, N. B. Smirnov, E. B. Yakimov, I. V. Shchemerov, A. V. Chernykh, A. I. Kochkova, A. A. Vasilev, F. Ren, P. H. Carey, S. J. Pearton, Appl. Phys. Lett. **115**, 032101 (2019).

- [16] A. Y. Polyakov, I. Lee, A. Miakonkikh, A. V. Chernykh, N. B. Smirnov, I. V. Shchemerov, A. I. Kochkova, A. A. Vasilev, S. J. Pearton, *J. Appl. Phys.* **127**, 175702 (2020).
- [17] A. Y. Polyakov, A. I. Kochkova, A. Azarov, V. Venkatachalapathy, A. V. Miakonkikh, A. A. Vasilev, A. V. Chernykh, I. V. Shchemerov, A. A. Romanov, A. Kuznetsov, S. J. Pearton, *J. Appl. Phys.* **133**, 095701 (2023).
- [18] A. Y. Polyakov, E. B. Yakimov, V. I. Nikolaev, A. I. Pechnikov, A. V. Miakonkikh, A. Azarov, I. Lee, A. A. Vasilev, A. I. Kochkova, I. V. Shchemerov, A. Kuznetsov, S. J. Pearton, *Crystals* **13**, 1400 (2023).
- [19] T. T. Huynh, E. Chikoidze, C. P. Irvine, M. Zakria, Y. Dumont, F. H. Teherani, E. V. Sandana, P. Bove, D. J. Rogers, M. R. Phillips, C. Ton-That, *Phys. Rev. Mater.* **4**, 085201 (2020).
- [20] A. Venzie, A. Portoff, E. C. P. Valenzuela, M. Stavola, W. B. Fowler, S. J. Pearton, E. R. Glaser, *J. Appl. Phys.* **131**, 035706 (2022).
- [21] Q. Jiang, J. Meng, Y. Shi, Z. Yin, J. Chen, J. Zhang, J. Wu, X. Zhang, *J. Semicond.* **43**, 092802, (2022).
- [22] Y. Shi, J. Meng, J. Chen, R. Wu, L. Zhang, J. Jiang, J. Deng, Z. Yin, X. Zhang, *J. Alloys Comp.* **974**, 172946 (2024).
- [23] H. Cui, H. F. Mohamed, C. Xia, Q. Sai, Wei Zhou, H. Qi, J. Zhao, J. Si, X. Ji, *J. Alloys Comp.* **788**, 925 (2019).

*Corresponding author: jjulye@126.com